Electronic Supplementary Material (ESI) for Dalton Transactions.
This journal is © The Royal Society of Chemistry 2020

Supporting Information

for

# Temperature-dependent hysteretic two-step spin crossover in two-dimensional Hofmann-type compounds

Yue Li,[a] Min Liu,*[b] Zi-Shuo Yao[c] and Jun Tao*[ac]

[a]*College of Chemistry and Chemical Engineering, Xiamen University, Xiamen 361005, Fujian Province, People's Republic of China. E-mail: taojun@bit.edu.cn*

[b]*School of Nuclear Science and Technology, University of South China, Hengyang 421001, Hunan Province, People's Republic of China. E-mail: liuquanusc@126.com*

[c]*Key Laboratory of Cluster Science of Ministry of Education, School of Chemistry and Chemical Engineering, Liangxiang Campus, Beijing Institute of Technology, Beijing 102488, People's Republic of China.*

Table S1. Crystal structure and refinement details for compound **1** at 298, 195, 85 K and **2** at 298, 190, 89 K.

| | Compound **1** | | | Compound **2** | | |
|---|---|---|---|---|---|---|
| Temp / K | 298 | 195 | 85 | 298 | 190 | 89 |
| formula | $FePdC_{28}N_8O_3H_{26}$ | $Fe_2Pd_2C_{56}N_{16}O_6H_{56}$ | $Fe_2Pd_2C_{56}N_{16}O_6H_{56}$ | $Fe_2Pt_2C_{56}N_{16}O_6H_{56}$ | $FePtC_{28}N_8O_3H_{26}$ | $FePtC_{28}N_8O_3H_{26}$ |
| $M_r$ | 684.82 | 1369.64 | 1369.64 | 1546.98 | 773.49 | 773.49 |
| cryst syst | | orthorhombic | | | orthorhombic | |
| space group | *Cmmm* | *Imma* | *Imma* | *Imma* | *Cmmm* | *Cmmm* |
| *a*, Å | 7.4125(6) | 7.2795(5) | 14.6772(11) | 7.4043(4) | 7.2305(3) | 7.1424(4) |
| *b*, Å | 28.588(3) | 14.9441(13) | 7.1611(4) | 15.1012(6) | 28.3930(14) | 28.216(3) |
| *c*, Å | 7.5142(6) | 28.394(2) | 28.221(2) | 28.6158(14) | 7.3865(5) | 7.3155(7) |
| $\alpha$, deg | 90 | 90 | 90 | 90 | 90 | 90 |
| $\beta$, deg | 90 | 90 | 90 | 90 | 90 | 90 |
| $\gamma$, deg | 90 | 90 | 90 | 90 | 90 | 90 |
| $V$, Å$^3$ | 1592.3(2) | 3088.8(4) | 2966.2(3) | 3199.6(3) | 1516.42 | 1474.3(2) |
| $Z$ | 2 | 2 | 2 | 2 | 2 | 2 |
| $D_c$, g cm$^{-3}$ | 1.316 | 1.356 | 1.412 | 1.494 | 1.576 | 1.621 |
| $\mu$, mm$^{-1}$ | 1.048 | 1.080 | 1.125 | 4.848 | 5.115 | 5.261 |
| $F$(000) | 632 | 1264 | 1264 | 1392 | 696 | 696 |
| goodness-of-fit on $F^2$ | 1.014 | 1.177 | 1.169 | 1.060 | 1.067 | 1.132 |
| $R1$ ($I \geq 2\sigma(I)$)[a] | 0.0345 | 0.0741 | 0.0572 | 0.0348 | 0.0451 | 0.0295 |
| $wR2$ (all data)[a] | 0.0892 | 0.1827 | 0.1481 | 0.0874 | 0.1176 | 0.0752 |

a: $I \geq 2\sigma(I)$: $R1 = \sum||F_o| - |F_c||/\sum|F_o|$, $wR_2 = \{\sum[w(F_o^2 - F_c^2)^2]/\sum[w(F_o^2)^2]\}^{1/2}$.

Table S2. The $Fe^{II}$–N bond lengths in compounds **1** and **2** at different temperatures.

| | **1** | | | **2** | | |
|---|---|---|---|---|---|---|
| *T* / K | 298 | 195 | 85 | 298 | 190 | 89 |
| Fe–N1 (Å) | 2.195(3) | 2.120(4) | 2.033(5) | 2.206(3) | 2.084(7) | 2.020(4) |
| Fe–N3 (Å) | 2.146(3) | 2.068(5) | 1.983(4) | 2.160(4) | 2.027(7) | 1.966(4) |
| Fe–$N_{ave}$ (Å) | 2.170(8) | 2.094(45) | 2.008(45) | 2.183(35) | 2.056(2) | 1.993(4) |

Table S3. Fe···Fe distances in compounds **1** and **2** at different temperatures.

| | **1** | | | **2** | | |
|---|---|---|---|---|---|---|
| *T* / K | 298 | 195 | 85 | 298 | 190 | 89 |
| $d_1$ (Å) | 7.51(4) | 7.47(2) | 7.33(9) | 7.55(1) | 7.38(7) | 7.31(6) |
| $d_2$ (Å) | 7.41(2) | 7.27(9) | 7.16(1) | 7.40(4) | 7.23(1) | 7.14(2) |
| $d_{ave}$ (Å) | 7.46(3) | 7.37(55) | 7.25 | 7.47(75) | 7.30(9) | 7.22(9) |

Table S4. The π···π interactions and the distortion parameter $\Sigma_{Fe}$ of {$FeN_6$} moiety at different temperatures for compounds **1** and **2**.

| | **1** | | | **2** | | |
|---|---|---|---|---|---|---|
| *T* / K | 298 | 195 | 85 | 298 | 190 | 89 |
| π···π interations (Å) | 3.771(9) | 3.692(11) | 3.653(8) | 3.732(12) | 3.673(17) | 3.653(9) |
| $\Sigma_{Fe}$ of {$FeN_6$} (°) | | | | | | |
| $\sum_{i=1}^{12}\lvert\varphi_i - 90°\rvert$ | 30.7(26) | 44.2(7) | 37.0 | 28.4 | 37.6 | 32.8 |

Table S5. The pore sizes in compound **1** and **2** at different temperature.

| | | 1 | | | 2 | | |
|---|---|---|---|---|---|---|---|
| *T* / K | | 298 | 195 | 85 | 298 | 190 | 89 |
| pore size | A | 14.294 × 3.572 | 14.144 × 3.084 | 14.110 × 2.837 | 14.308 × 3.786 | 14.196 × 3.420 | 14.108 × 3.505 |
| | B | 14.294 × 3.572 | 14.144 × 3.898 | 14.110 × 3.931 | 14.308 × 4.295 | 14.196 × 3.420 | 14.108 × 3.505 |

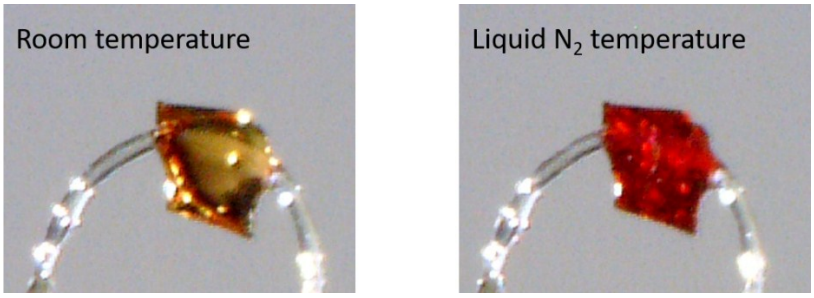


**Fig. S1.** Thermochromism of compound **1**.

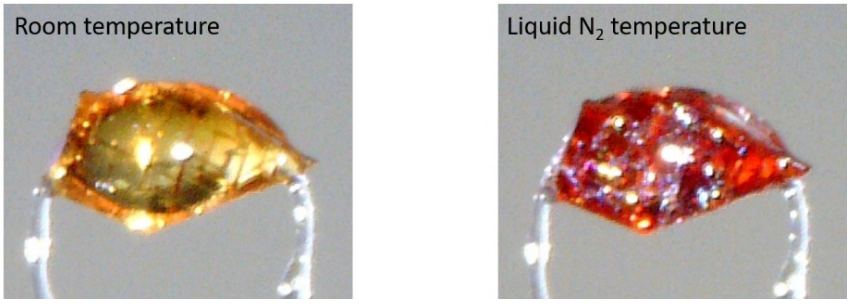


**Fig. S2.** Thermochromism of compound **2**.

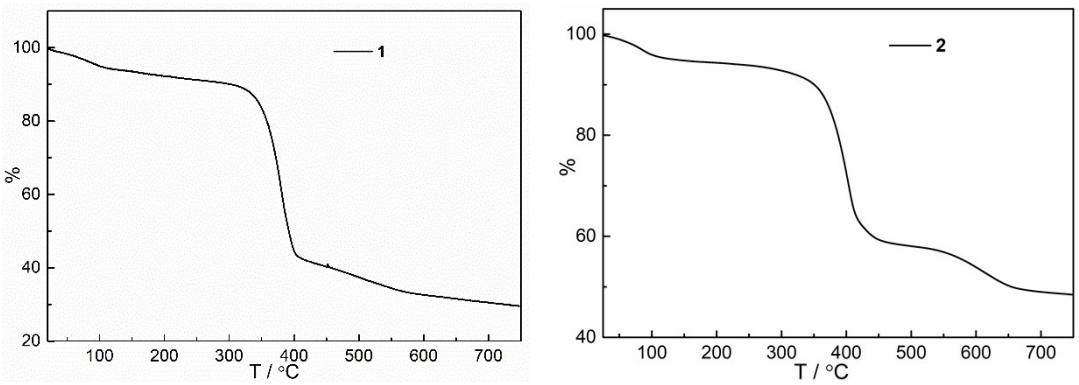


**Fig. S3.** TGA of compounds **1** and **2**.

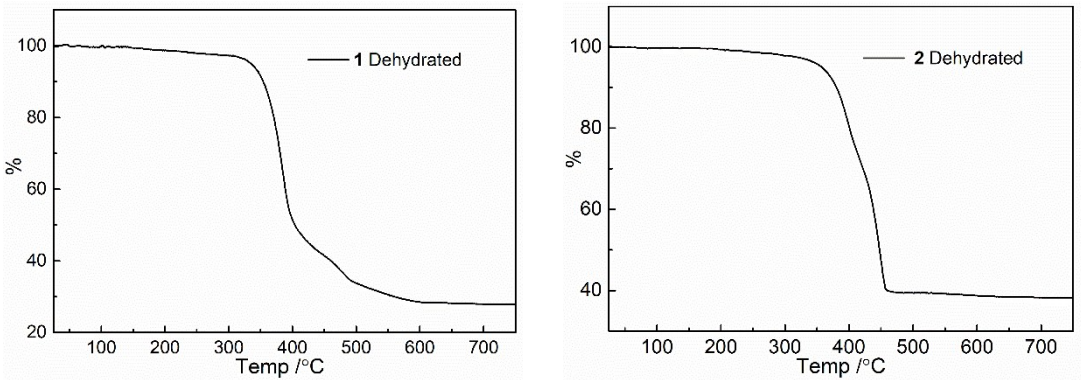


**Fig. S4.** TGA of dehydrated **1** and **2**.

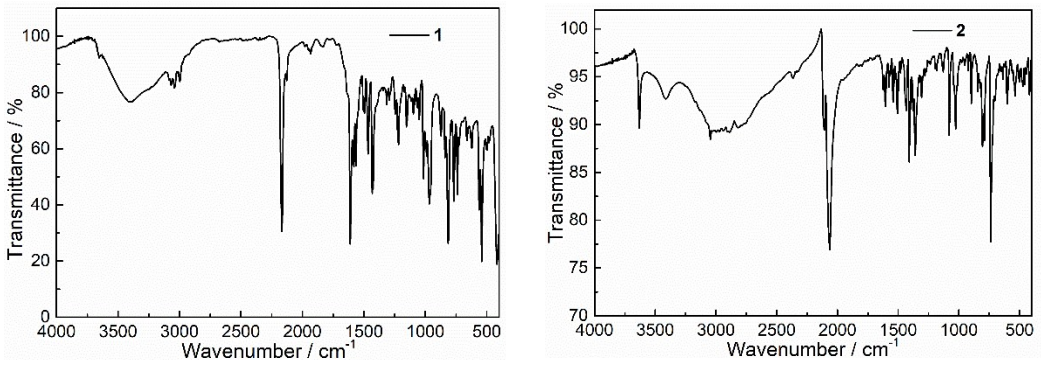


**Fig. S5.** The FT-IR spectra of **1** and **2**.

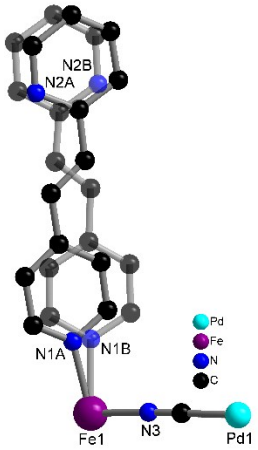


**Fig. S6.** The asymmetric unit of compound **1** at 195 K.

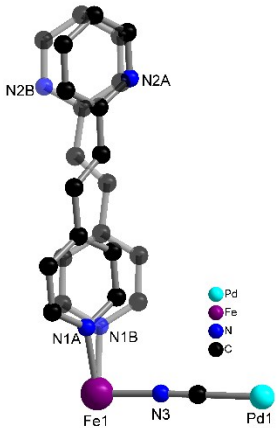


**Fig. S7.** The asymmetric unit of compound **1** at 85 K.

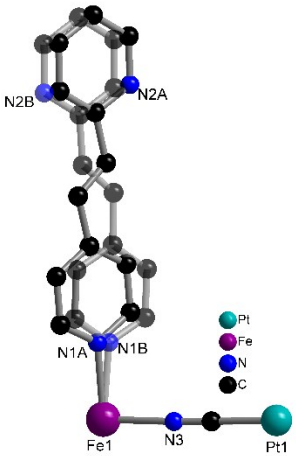


**Fig. S8.** The asymmetric unit of compound **2** at 298 K.

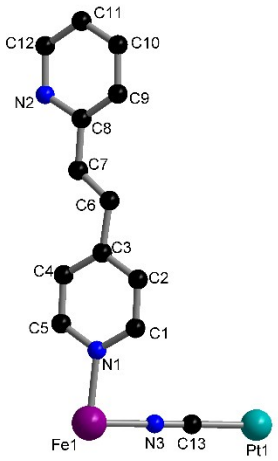


**Fig. S9.** The asymmetric unit of compound **2** at 190 K.

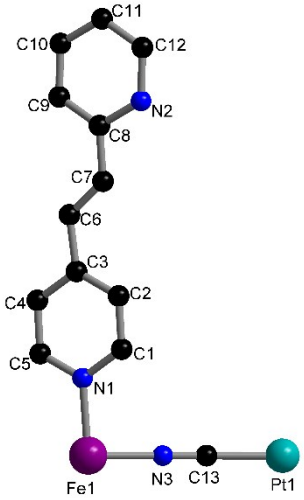


**Fig. S10.** The asymmetric unit of compound **2** at 89 K.